
# Search for Spatially Extended *Fermi*-LAT Sources Using Two Years of Data

Joshua Lande,
Stefan Funk,
Markus Ackermann

February 15, 2012

**Search for Spatially Extended *Fermi*-LAT Sources Using Two Years of Data**

J. Lande[1,2], M. Ackermann[3,4], A. Allafort[1], J. Ballet[5], K. Bechtol[1], T. H. Burnett[6], J. Cohen-Tanugi[7], A. Drlica-Wagner[1], S. Funk[1,8], F. Giordano[9,10], M.-H. Grondin[11,12], M. Kerr[1], M. Lemoine-Goumard[13,14]

- Cat II paper
- Internal referees: Marianne Lemoine-Goumard + Johann Cohen-Tanugi (+ unofficially Jean Ballet)
- Submitted to ApJ

# Section 2.1. Modeling Extended Sources in the `pointlike` Package

New method to study spatially-extended *Fermi*-LAT sources

- Description of `pointlike`
- Implementation of extended sources
- Simultaneously Fit position + extension
- speed up likelihood computation
- Cross check TS + spectral values using `gtlike`

# Fig. 2: LAT PSF

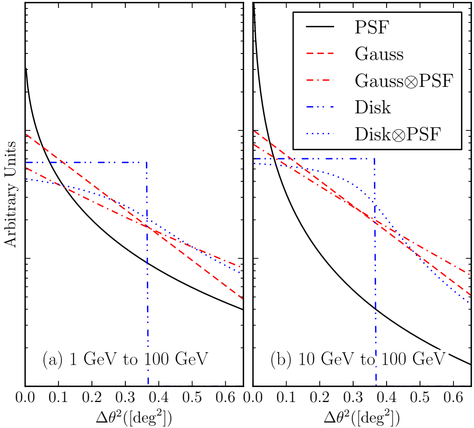
PSF
Gauss
Gauss⊗PSF
Disk
Disk⊗PSF
Arbitrary Units
(a) 1 GeV to 100 GeV
(b) 10 GeV to 100 GeV
0.0 0.1 0.2 0.3 0.4 0.5 0.6
0.0 0.1 0.2 0.3 0.4 0.5 0.6
Δθ²([deg²])
Δθ²([deg²])

# Table 1: False-Detection Rate

Table 1. Monte Carlo Spectral Parameters

| Spectral Index | Flux[a] ($\mathrm{ph\,cm^{-2}\,s^{-1}}$) | $N_{1-100\mathrm{GeV}}$ | $\langle\mathrm{TS}\rangle_{1-100\mathrm{GeV}}$ | $N_{10-100\mathrm{GeV}}$ | $\langle\mathrm{TS}\rangle_{10-100\mathrm{GeV}}$ |
|---|---|---|---|---|---|
| 1.5 | $3\times10^{-7}$ | 18938 | 22233 | 18938 | 8084 |
| | $10^{-7}$ | 19079 | 5827 | 19079 | 2258 |
| | $3\times10^{-8}$ | 19303 | 1276 | 19303 | 541 |
| | $10^{-8}$ | 19385 | 303 | 19381 | 142 |
| | $3\times10^{-9}$ | 18694 | 62 | 12442 | 43 |
| 2 | $10^{-6}$ | 18760 | 22101 | 18760 | 3033 |
| | $3\times10^{-7}$ | 18775 | 4913 | 18775 | 730 |
| | $10^{-7}$ | 18804 | 1170 | 18803 | 192 |
| | $3\times10^{-8}$ | 18836 | 224 | 15256 | 50 |
| | $10^{-8}$ | 17060 | 50 | ··· | ··· |
| 2.5 | $3\times10^{-6}$ | 18597 | 19036 | 18597 | 786 |
| | $10^{-6}$ | 18609 | 4738 | 18608 | 208 |
| | $3\times10^{-7}$ | 18613 | 954 | 15958 | 53 |
| | $10^{-7}$ | 18658 | 203 | ··· | ··· |
| | $3\times10^{-8}$ | 14072 | 41 | ··· | ··· |
| 3 | $10^{-5}$ | 18354 | 19466 | 18354 | 215 |
| | $3\times10^{-6}$ | 18381 | 4205 | 15973 | 54 |
| | $10^{-6}$ | 18449 | 966 | ··· | ··· |
| | $3\times10^{-7}$ | 18517 | 174 | ··· | ··· |
| | $10^{-7}$ | 13714 | 41 | ··· | ··· |

[a] Integral 100 MeV to 100 GeV flux.

- Simulate point-like sources
- Test for extension
- Good agreement with Wilk's Theorem
- Use $\sqrt{\mathrm{TS}_{\mathrm{ext}}}$ as a measure of significance
- $\sim 20,000$ Simulations per spectral model!
- Test in 1 GeV to 100 GeV + 10 GeV to 100 GeV energy range

# Fig. 3+4: False-Detection Rate (cont)

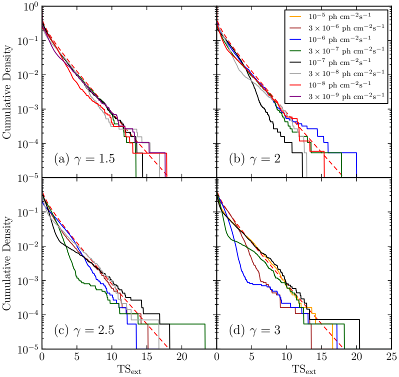


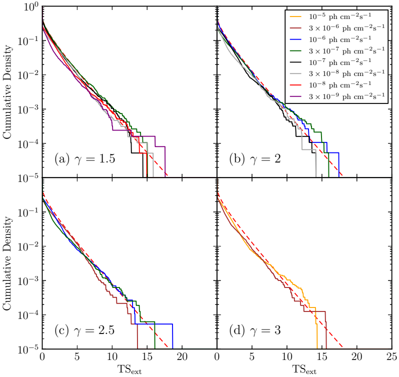

# Fig. 5: Detection Threshold

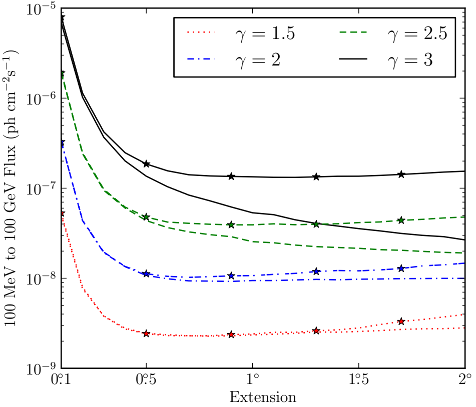


- Detetion threshold to extension
- $\langle \mathrm{TS}_{\mathrm{ext}} \rangle = 16$
- Vary spectra, background, energy range
- Overlay extended sources
- Reference for future publications!

# Fig. 6: Detection Threshold (cont)

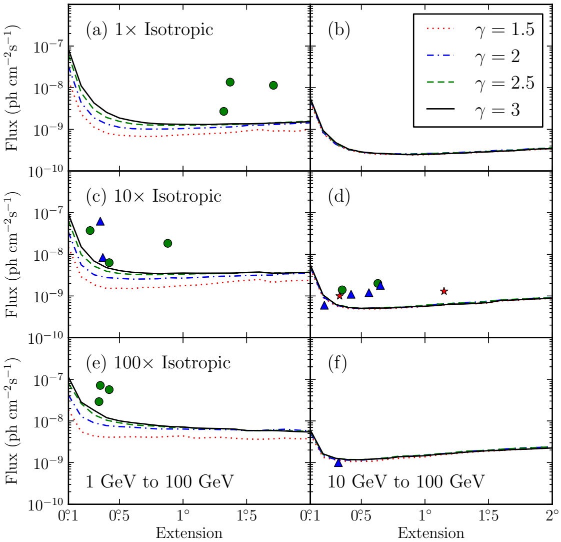


- Compute sensitivty for different background levels, energy ranges.

Table 2. Extension Detection Threshold

| $\gamma$ | BG | 0.1 | 0.2 | 0.3 | 0.4 | 0.5 | 0.6 | 0.7 | 0.8 | 0.9 | 1.0 | 1.1 | 1.2 | 1.3 | 1.4 | 1.5 | 1.6 | 1.7 | 1.8 | 1.9 | 2.0 |
|---|---|---|---|---|---|---|---|---|---|---|---|---|---|---|---|---|---|---|---|---|---|
| | | | | | | | | | | E>1 GeV | | | | | | | | | | | |
| 1.5 | 1× | 148.1 | 23.3 | 11.3 | 8.0 | 7.2 | 6.9 | 6.7 | 6.8 | 7.1 | 7.4 | 7.6 | 7.9 | 8.1 | 8.5 | 9.2 | 9.9 | 9.1 | 9.2 | 9.0 | 10.3 |
| | 10× | 148.4 | 29.0 | 18.7 | 15.2 | 15.4 | 15.0 | 16.1 | 16.0 | 16.8 | 17.7 | 18.2 | 19.3 | 20.9 | 22.5 | 23.8 | 24.8 | 21.3 | 22.8 | 23.4 | 23.7 |
| | 100× | 186.8 | 55.0 | 43.4 | 40.7 | 41.0 | 41.8 | 40.9 | 40.9 | 42.7 | 43.6 | 38.4 | 39.9 | 40.6 | 38.4 | 36.9 | 36.3 | 37.1 | 38.8 | 37.2 | 37.6 |
| 2 | 1× | 328.4 | 43.4 | 18.9 | 13.4 | 11.2 | 10.4 | 10.2 | 10.2 | 10.2 | 10.4 | 10.7 | 10.9 | 11.2 | 11.5 | 12.4 | 12.6 | 13.0 | 13.4 | 14.0 | 14.4 |
| | 10× | 341.0 | 55.9 | 32.3 | 27.6 | 26.5 | 25.4 | 25.6 | 25.9 | 27.4 | 26.8 | 27.8 | 28.7 | 29.8 | 30.1 | 31.0 | 31.5 | 31.7 | 34.0 | 34.3 | 35.9 |
| | 100× | 420.5 | 128.3 | 90.2 | 77.3 | 73.3 | 70.8 | 67.5 | 64.3 | 64.2 | 64.1 | 62.8 | 63.6 | 61.7 | 61.9 | 58.4 | 59.0 | 61.4 | 63.3 | 60.1 | 58.1 |
| 2.5 | 1× | 627.1 | 75.6 | 29.8 | 19.3 | 15.5 | 13.5 | 12.8 | 12.6 | 12.5 | 12.5 | 12.6 | 12.9 | 12.9 | 13.1 | 13.5 | 13.7 | 14.3 | 14.8 | 15.2 | 15.8 |
| | 10× | 638.9 | 99.1 | 52.1 | 39.1 | 34.6 | 33.0 | 32.5 | 32.5 | 32.8 | 33.2 | 34.1 | 34.3 | 34.5 | 35.1 | 36.6 | 36.9 | 35.5 | 36.0 | 36.5 | 37.3 |
| | 100× | 795.0 | 262.1 | 140.9 | 104.3 | 90.4 | 81.2 | 77.2 | 75.1 | 69.7 | 70.9 | 66.5 | 65.6 | 64.9 | 64.0 | 58.9 | 58.1 | 60.2 | 58.4 | 57.5 | 55.8 |
| 3 | 1× | 841.5 | 110.6 | 43.2 | 25.5 | 18.7 | 16.1 | 14.4 | 13.6 | 13.3 | 13.2 | 13.1 | 13.1 | 13.4 | 13.6 | 13.5 | 13.8 | 14.2 | 14.4 | 14.8 | 15.4 |
| | 10× | 921.6 | 151.3 | 69.1 | 47.8 | 40.7 | 37.1 | 35.5 | 34.5 | 35.1 | 35.5 | 35.3 | 35.3 | 35.4 | 35.5 | 36.8 | 37.6 | 35.3 | 35.4 | 36.3 | 36.6 |
| | 100× | 1124.1 | 282.9 | 181.1 | 119.8 | 100.7 | 91.1 | 84.3 | 77.9 | 73.3 | 71.8 | 67.6 | 66.4 | 65.5 | 63.9 | 59.0 | 58.6 | 58.8 | 57.5 | 55.4 | 54.4 |
| | | | | | | | | | | E>10 GeV | | | | | | | | | | | |
| 1.5 | 1× | 44.6 | 8.0 | 4.3 | 3.2 | 2.7 | 2.6 | 2.5 | 2.5 | 2.4 | 2.5 | 2.5 | 2.6 | 2.7 | 2.8 | 2.9 | 2.9 | 3.1 | 3.2 | 3.3 | 3.4 |
| | 10× | 45.2 | 9.2 | 5.8 | 5.0 | 4.9 | 4.9 | 5.0 | 5.2 | 5.3 | 5.7 | 5.9 | 6.3 | 6.6 | 6.5 | 6.8 | 7.6 | 7.8 | 8.2 | 8.5 | 8.7 |
| | 100× | 47.3 | 13.4 | 11.6 | 10.6 | 10.8 | 10.8 | 12.0 | 12.7 | 13.2 | 13.7 | 15.3 | 16.1 | 17.2 | 18.2 | 18.9 | 19.5 | 20.4 | 21.0 | 21.7 | 22.9 |
| 2 | 1× | 49.7 | 8.4 | 4.4 | 3.3 | 2.8 | 2.6 | 2.6 | 2.6 | 2.6 | 2.6 | 2.7 | 2.7 | 2.8 | 2.9 | 3.0 | 3.2 | 3.2 | 3.4 | 3.5 | 3.5 |
| | 10× | 48.6 | 9.5 | 6.0 | 5.2 | 5.0 | 5.2 | 5.2 | 5.3 | 5.4 | 5.8 | 6.4 | 6.6 | 7.0 | 7.1 | 7.5 | 8.0 | 8.3 | 8.6 | 9.0 | 9.2 |
| | 100× | 51.8 | 14.7 | 11.8 | 11.5 | 11.5 | 11.9 | 13.2 | 14.0 | 14.3 | 15.3 | 16.2 | 16.9 | 18.4 | 19.2 | 19.8 | 21.0 | 22.0 | 22.8 | 23.2 | 24.3 |
| 2.5 | 1× | 53.1 | 9.1 | 4.5 | 3.3 | 2.8 | 2.7 | 2.6 | 2.5 | 2.5 | 2.6 | 2.7 | 2.7 | 2.8 | 2.8 | 2.9 | 3.1 | 3.2 | 3.3 | 3.5 | 3.6 |
| | 10× | 53.7 | 10.5 | 6.3 | 5.4 | 5.1 | 5.1 | 5.3 | 5.4 | 5.7 | 6.0 | 6.3 | 6.6 | 6.8 | 6.9 | 7.5 | 8.1 | 8.3 | 8.6 | 8.9 | 9.2 |
| | 100× | 57.0 | 15.6 | 12.7 | 11.9 | 11.8 | 12.2 | 13.1 | 14.3 | 14.6 | 15.2 | 16.3 | 17.0 | 18.8 | 19.2 | 19.9 | 21.0 | 21.9 | 22.3 | 23.3 | 23.7 |
| 3 | 1× | 55.5 | 9.4 | 4.8 | 3.4 | 2.9 | 2.7 | 2.6 | 2.5 | 2.5 | 2.5 | 2.6 | 2.7 | 2.7 | 2.8 | 2.9 | 3.0 | 3.1 | 3.2 | 3.4 | 3.4 |
| | 10× | 56.0 | 10.5 | 6.2 | 5.3 | 5.1 | 5.1 | 5.1 | 5.3 | 5.5 | 5.7 | 5.9 | 6.4 | 6.4 | 6.6 | 7.0 | 7.8 | 8.0 | 8.3 | 8.6 | 8.9 |
| | 100× | 60.3 | 16.2 | 12.7 | 11.7 | 11.8 | 12.2 | 12.6 | 13.8 | 14.2 | 14.6 | 15.8 | 16.5 | 17.6 | 18.5 | 19.4 | 19.8 | 20.7 | 21.0 | 21.8 | 22.5 |

Note. — The detection threshold to resolve spatially extended sources with a uniform disk spatial model for a two-year exposure The threshold is calculated for sources of varying energy ranges, spectral indices, and background levels. The sensitivity was calculated against a Sreekumar-like isotropic background and the second column is the factor that the simulated background was scaled by. The remaining columns are varying sizes of the source. The table quotes integral fluxes in the analyzed energy range (1 GeV to 100 GeV or 10 GeV to 100 GeV) in units of $10^{-10}\ \mathrm{ph\,cm^{-2}\,s^{-1}}$.

# Fig. 7: Detection Threshold (cont)

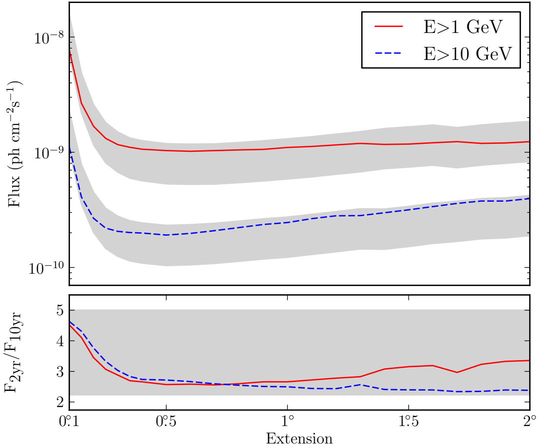


- Compute sensitivty after 10 years.

# Fig. 8: Effects of Source Confusion

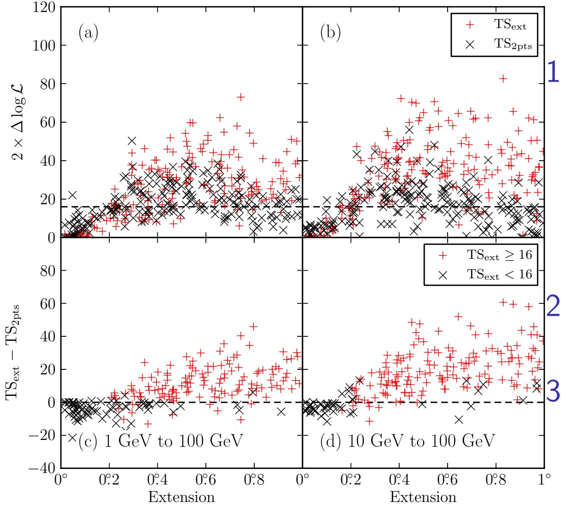


1. Non-nested model comparison

   $$\mathrm{TS}_{\mathrm{2pts}} = 2\log(\mathcal{L}_{\mathrm{2pts}}/\mathcal{L}_{\mathrm{ps}})$$

2. Simulate extended sources.
3. Fit as point-like sources.

# Fig. 9: Effects of Source Confusion (cont)

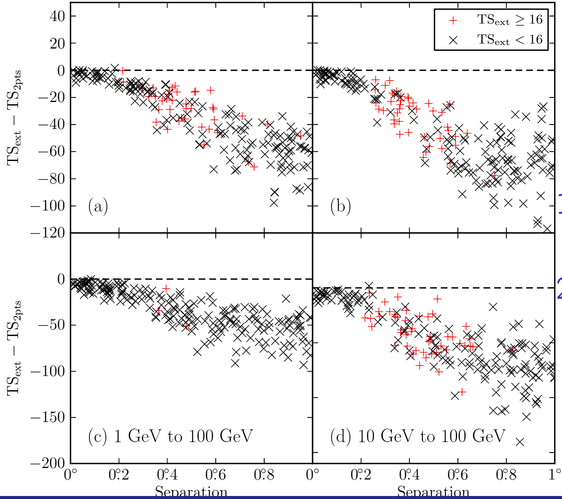


1. Simulate point-like sources.
2. Fit for extension.

# Fig. 10: $TS_{EXT}$ for 2LAC AGN

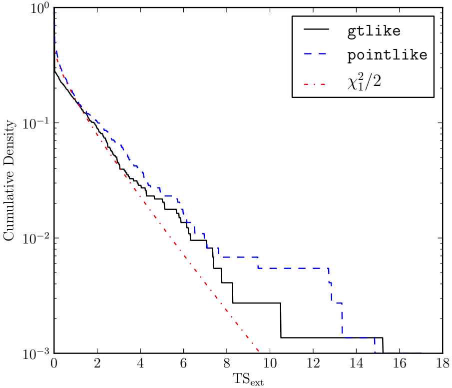


- Use point-like AGN to validate extended source analysis
- Test clean 2LAC AGN for extension
- Don't find AGN to be extended!

# Fig. 1: IC 443

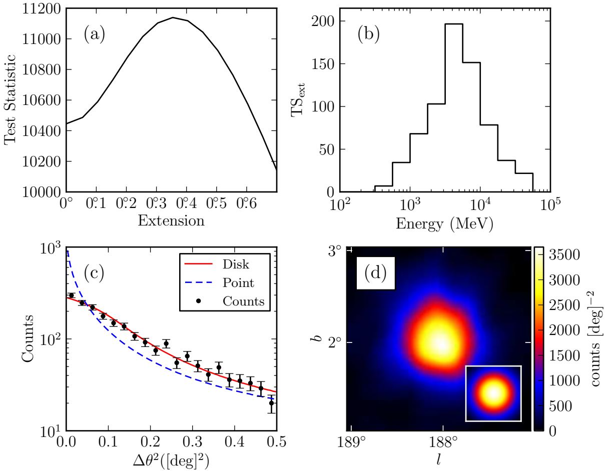
(a)
Test Statistic
11200
11000
10800
10600
10400
10200
10000
0° 0.°1 0.°2 0.°3 0.°4 0.°5 0.°6
Extension
(b)
$TS_{ext}$
200
150
100
50
0
$10^2$ $10^3$ $10^4$ $10^5$
Energy (MeV)
(c)
Counts
Disk
Point
Counts
$10^3$
$10^2$
$10^1$
0.0 0.1 0.2 0.3 0.4 0.5
$\Delta\theta^2([\mathrm{deg}]^2)$
(d)
$b$
3°
2°
189° 188°
$l$
3500
3000
2500
2000
1500
1000
500
0
counts $[\mathrm{deg}]^{-2}$

# Fig. 11: Residual TS Map

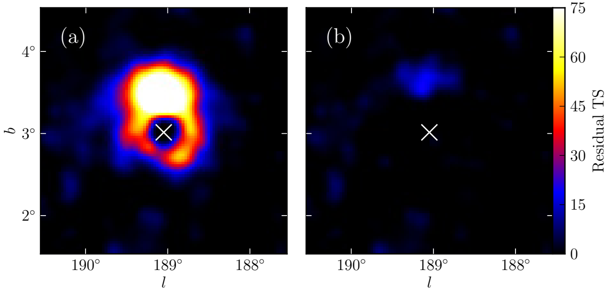

# Table 3: extended sources in 2FGL

Table 3. Analysis of the twelve extended sources included in 2FGL

| Name | GLON (deg.) | GLAT (deg.) | $\sigma$ (deg.) | TS | $TS_{ext}$ | Pos Err (deg.) | Flux[(a)] | Index |
|---|---|---|---|---|---|---|---|---|
| | | | E>1 GeV | | | | | |
| SMC | 302.59 | -44.42 | $1.32 \pm 0.15 \pm 0.31$ | 95.0 | 52.9 | 0.14 | $2.7 \pm 0.3$ | $2.48 \pm 0.19$ |
| LMC | 279.26 | -32.31 | $1.37 \pm 0.04 \pm 0.11$ | 1127.9 | 909.9 | 0.04 | $13.6 \pm 0.6$ | $2.43 \pm 0.06$ |
| IC443 | 189.05 | 3.04 | $0.35 \pm 0.01 \pm 0.04$ | 10692.9 | 554.4 | 0.01 | $62.4 \pm 1.1$ | $2.22 \pm 0.02$ |
| Vela X | 263.34 | -3.11 | 0.88 | | | | | |
| Centaurus A | 309.52 | 19.42 | $\sim 10$ | | | | | |
| W28 | 6.50 | -0.27 | $0.42 \pm 0.02 \pm 0.05$ | 1330.8 | 163.8 | 0.01 | $56.5 \pm 1.8$ | $2.60 \pm 0.03$ |
| W30 | 8.61 | -0.20 | $0.34 \pm 0.02 \pm 0.02$ | 464.8 | 76.0 | 0.02 | $29.1 \pm 1.5$ | $2.56 \pm 0.05$ |
| W44 | 34.69 | -0.39 | $0.35 \pm 0.02 \pm 0.02$ | 1917.0 | 224.8 | 0.01 | $71.2 \pm 0.5$ | $2.66 \pm 0.00$ |
| W51C | 49.12 | -0.45 | $0.27 \pm 0.02 \pm 0.04$ | 1823.4 | 118.9 | 0.01 | $37.2 \pm 1.3$ | $2.34 \pm 0.03$ |
| Cygnus Loop | 74.21 | -8.48 | $1.71 \pm 0.05 \pm 0.06$ | 357.9 | 246.0 | 0.06 | $11.4 \pm 0.7$ | $2.50 \pm 0.10$ |
| | | | E>10 GeV | | | | | |
| MSH15−52 | 320.39 | -1.22 | $0.21 \pm 0.04 \pm 0.04$ | 76.3 | 6.6 | 0.03 | $0.6 \pm 0.1$ | $2.20 \pm 0.22$ |
| HESS J1825−137 | 17.57 | -0.45 | $0.65 \pm 0.04 \pm 0.02$ | 82.9 | 44.9 | 0.05 | $1.8 \pm 0.8$ | $1.83 \pm 0.73$ |

[(a)]Integral Flux in units of $10^{-9}$ ph cm$^{-2}$ s$^{-1}$ and integrated in the fit energy range (either 1 GeV to 100 GeV or 10 GeV to 100 GeV).

Note. — All sources were fit using a spatial model assuming a uniform radially symmetric intensity distribution. GLON and GLAT are Galactic longitude and latitude of the best fit extended source respectively. The first error on $\sigma$ is statistical and the second is systematic (see Section 8). The errors on the integral fluxes and the spectral indices are statistical only. Pos Err is the error on the position of the source. Vela X and the Centaurus A Lobes were not fit in our analysis but are include for completeness.

- Test 12 extended 2FGL sources for extension
- Systematic reanalysis using 2 years of data.
- Assume uniform disk
- Extended sources are extended!

# Section 9: Extended Source Search

- Run a dedicated search
- Find previously-unresolved extended 2FGL sources
- Search for $E > 1$ GeV and $E > 10$ GeV
- Many difficulties in search, discussed at length in text...
- Publish only good candidates

# Fig. 12: Systematics in the plane

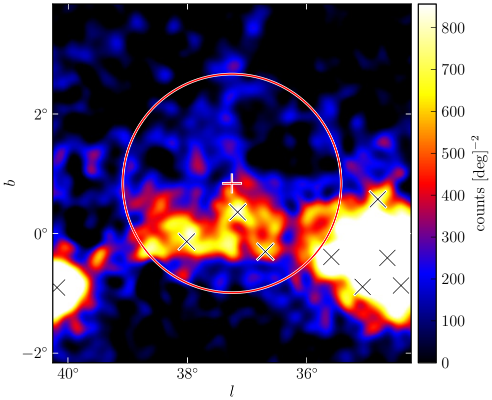

# Table 4: New extended Sources

Table 4. Extension fit for the nine additional extended sources

| Name | GLON (deg.) | GLAT (deg.) | $\sigma$ (deg.) | TS | $TS_{ext}$ | Pos Err (deg.) | Flux[(a)] | Index | Counterpart |
|---|---|---|---|---|---|---|---|---|---|
| E>1 GeV | | | | | | | | | |
| 2FGL J0823.0−4246 | 260.32 | −3.28 | $0.37 \pm 0.03 \pm 0.02$ | 322.2 | 48.0 | 0.02 | $8.4 \pm 0.6$ | $2.21 \pm 0.09$ | Puppis A |
| 2FGL J1627.0−2425c | 353.07 | 16.80 | $0.42 \pm 0.05 \pm 0.16$ | 139.9 | 32.4 | 0.04 | $6.3 \pm 0.6$ | $2.50 \pm 0.14$ | Ophiuchus |
| E>10 GeV | | | | | | | | | |
| 2FGL J0851.7−4635 | 266.31 | −1.43 | $1.15 \pm 0.08 \pm 0.02$ | 116.6 | 86.8 | 0.07 | $1.3 \pm 0.2$ | $1.74 \pm 0.21$ | Vela Jr. |
| 2FGL J1615.0−5051 | 332.37 | −0.13 | $0.32 \pm 0.04 \pm 0.01$ | 50.4 | 16.7 | 0.04 | $1.0 \pm 0.2$ | $2.19 \pm 0.28$ | HESS J1616−508 |
| 2FGL J1615.2−5138 | 331.66 | −0.66 | $0.42 \pm 0.04 \pm 0.02$ | 76.1 | 46.5 | 0.04 | $1.1 \pm 0.2$ | $1.79 \pm 0.26$ | HESS J1614−518 |
| 2FGL J1632.4−4753c | 336.52 | 0.12 | $0.35 \pm 0.04 \pm 0.02$ | 64.4 | 26.9 | 0.04 | $1.4 \pm 0.2$ | $2.66 \pm 0.30$ | HESS J1632−478 |
| 2FGL J1712.4−3941[(b)] | 347.26 | −0.53 | $0.56 \pm 0.04 \pm 0.02$ | 59.4 | 38.5 | 0.05 | $1.2 \pm 0.2$ | $1.87 \pm 0.22$ | RX J1713.7−3946 |
| 2FGL J1837.3−0700c | 25.08 | 0.13 | $0.33 \pm 0.07 \pm 0.05$ | 47.0 | 18.5 | 0.07 | $1.0 \pm 0.2$ | $1.65 \pm 0.29$ | HESS J1837−069 |
| 2FGL J2021.5+4026 | 78.24 | 2.20 | $0.63 \pm 0.05 \pm 0.04$ | 237.2 | 128.9 | 0.05 | $2.0 \pm 0.2$ | $2.42 \pm 0.19$ | $\gamma$-Cygni |

[(a)]Integral Flux in units of $10^{-9}$ ph cm$^{-2}$ s$^{-1}$ and integrated in the fit energy range (either 1 GeV to 100 GeV or 10 GeV to 100 GeV).

[(b)]The discrepancy in the best fit spectra of 2FGL J1712.4−3941 compared to Abdo et al. (2011e) is due to fitting over a different energy range.

- 6 new extended sources
- + RX J1713-3946 & Vela Jr (not extended in 2FGL)
- + 1 source in Ophiuchus region → diffuse emission

# Section 8: Extension Systematics

Test systematics due to not knowing PSF

- Compare best fit extension to MC based PSF
- Use difference as systematic
- Small effect on extension, large effect on statistical significance
- Probably too conservative. . .

Test systematics due to not knowing PSF

- Break up GALPROP diffuse model into multiple components
- Fit each component locally
- Tests systematics due to imperfect diffuse modeling

# Table 5: Dual Localization, alternative PSF, alternative Diffuse

Table 5. Dual localization, alternative PSF, and alternative approach to modeling the diffuse emission

| Name | $TS_{\texttt{pointlike}}$ | $TS_{\texttt{gtlike}}$ | $TS_{\text{alt,diff}}$ | $TS_{\text{ext}\texttt{pointlike}}$ | $TS_{\text{ext}\texttt{gtlike}}$ | $TS_{\text{extalt,diff}}$ | $\sigma$ (deg.) | $\sigma_{\text{alt,diff}}$ (deg.) | $\sigma_{\text{alt,psf}}$ (deg.) | $TS_{\text{2pts}}$ |
|---|---|---|---|---|---|---|---|---|---|---|
| | | | | E>1 GeV | | | | | | |
| 2FGL J0823.0−4246 | 331.9 | 322.2 | 356.0 | 60.0 | 48.0 | 56.0 | 0.37 | 0.39 | 0.39 | 23.0 |
| 2FGL J1627.0−2425c | 154.8 | 139.9 | 105.7 | 39.4 | 32.4 | 24.8 | 0.42 | 0.40 | 0.58 | 24.5 |
| | | | | E>10 GeV | | | | | | |
| 2FGL J0851.7−4635 | 115.2 | 116.6 | 123.1 | 83.9 | 86.8 | 89.8 | 1.15 | 1.16 | 1.17 | 15.5 |
| 2FGL J1615.0−5051[a] | 48.2 | 50.4 | 56.6 | 15.2 | 16.7 | 17.8 | 0.32 | 0.33 | 0.32 | 13.1 |
| 2FGL J1615.2−5138 | 75.0 | 76.1 | 83.8 | 42.9 | 46.5 | 54.1 | 0.42 | 0.43 | 0.43 | 35.1 |
| 2FGL J1632.4−4753c | 64.5 | 64.4 | 66.8 | 23.0 | 26.9 | 25.5 | 0.35 | 0.36 | 0.37 | 10.9 |
| 2FGL J1712.4−3941 | 59.8 | 59.4 | 39.9 | 38.4 | 38.5 | 30.7 | 0.56 | 0.55 | 0.53 | 2.7 |
| 2FGL J1837.3−0700c | 44.5 | 47.0 | 39.2 | 17.6 | 18.5 | 16.1 | 0.33 | 0.32 | 0.38 | 10.8 |
| 2FGL J2021.5+4026 | 239.1 | 237.2 | 255.8 | 139.1 | 128.9 | 138.0 | 0.63 | 0.65 | 0.59 | 37.3 |

[a] Using `pointlike`, $TS_{\text{ext}}$ for 2FGL J1615.0−5051 was sligthly below 16 when the source was fit in the 10 GeV to 100 GeV energy range. To confirm the extension measure, the extension was refit in `pointlike` using a slightly lower energy. In the 5.6 GeV to 100 GeV energy range, we obtained a consistent extension and $TS_{\text{ext}}$ =28.0. In the rest of this paper, we quote the $E > 10$GeV results for consistency with the other sources.

## Puppis A

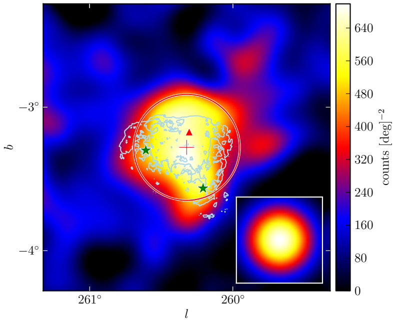


- X-ray contours
- Mid-aged SNR
- Not observed to directly interact with molecular clouds

## $\gamma$-Cygni

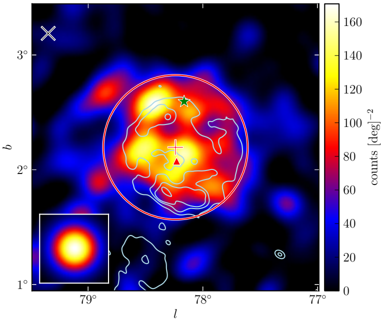


- Radio contours
- SNR interacting with molecular clouds?
- Veritas + Milagro detections

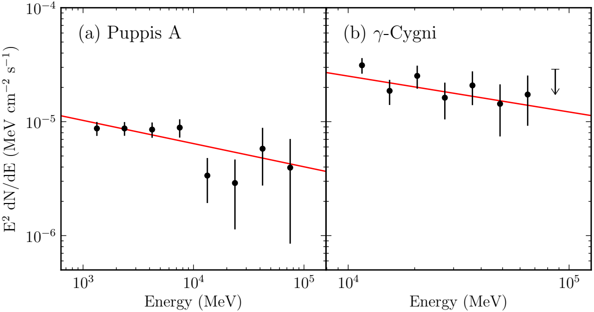

$10^{-4}$
$10^{-5}$
$10^{-6}$
E$^2$ dN/dE (MeV cm$^{-2}$ s$^{-1}$)
(a) Puppis A
$10^3$
$10^4$
$10^5$
Energy (MeV)
(b) $\gamma$-Cygni
$10^4$
$10^5$
Energy (MeV)

# Two Nearby LAT extended sources

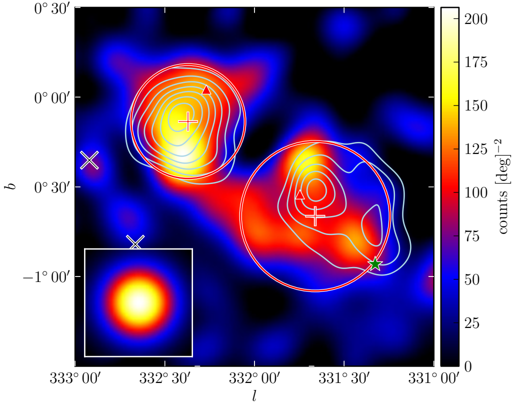


- (left): 2FGL J1615.0−5051
- Coincident with HESS J1616−508
- + X-ray pulsar PSR J1617−5055 + ∼ 1′ PWN
- PWN Candidate

- (right): 2FGL J1615.2−5138
- Coincident with HESS J1614−518
- No other compelling multiwavelenth counterpart

## 2FGL J1632.4−4753c

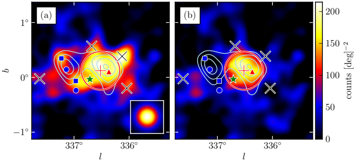


- Coincident with HESS J1632-478
- *XMM-Newton* point-like + extended emission
- (but no pulsations)
- PWN Candidate

## 2FGL J1837.3−0700c

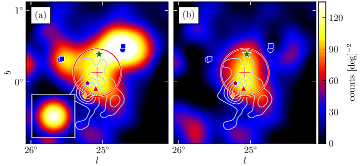


- Coincident with HESS J1837-069
- + X-ray pulsar PSR J1838−0655
- + $\sim 2'$ X-ray PWN
- PWN candidate
- Second X-ray PSR + PWN candidate in region (but no pulsations)

# Fig. 18: SED of HESS Sources

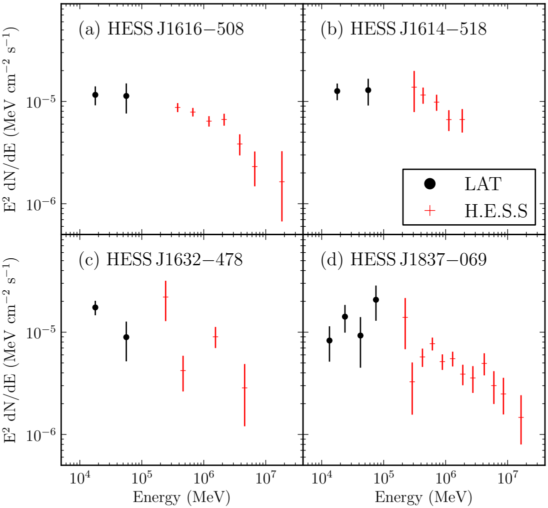

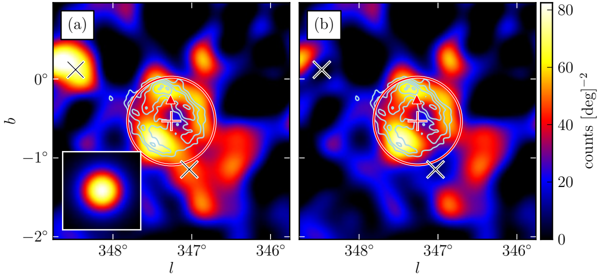
(a)
(b)
0°
−1°
−2°
b
348°
347°
346°
l
80
60
40
20
0
counts [deg]$^{-2}$

# Thank you

See text for more details:

- https://www-glast.stanford.edu/cgi-prot/pub_download?id=662